

Demonstration of a compact deep UV Raman spatial heterodyne spectrometer

Michael Foster,¹ William Brooks¹, Philipp Jahn²

¹ *IS-Instruments Ltd, Pipers Business Centre, 220 Vale Road, Tonbridge, Kent, TN9 1SP*

² *TOPTICA Photonics AG, Lochhamer Schlag 19, 82166 Graefelfing (Munich), Germany*

ABSTRACT

As Raman technology has advanced more challenging applications have been explored, where high fluorescence and low concentration of samples are present. Monoclonal antibodies and antibody fragments are increasingly important classes of biotherapeutics. However, these products are both challenging and expensive to manufacture. New process analytical tools (PAT) used to monitor these products during their manufacture are of significant interest. Deep UV Raman spectroscopy promises to provide the required specificity and accuracy, however instruments, have historically been large and complex. In this paper, a new deep UV Raman instrument is described which uses a solid-state laser and a spatial heterodyne spectrometer. The instrument overcomes practical limitations of the technique and could readily be used for online measurements. A series of observations of have been made of biopharmaceutical products, including IgG and domain antibodies where high levels of both specificity and accuracy has been demonstrated.

SCOPE

The technical report describes a new deep UV Raman instrument developed by IS-Instruments (ISI) and TOPTICA, and its first application to the measurement of biopharma products. The instrument performance is excellent acquiring spectra in a fraction of the time compared to existing systems, while its stability, compactness and ease of use are a game changer in terms of deep UV systems. In this note, a general description of the instrument is provided together with a test campaign examining products including IgG and antibody fragments.

For more information, please contact ISI at info@is-instruments.com directly or the authors of the document.

INTRODUCTION

For over a decade, Raman spectroscopy has been identified as a potential measurement technique for application in biologics production. The method is non-invasive and, in principle, can be used to measure any molecular compound providing high specificity and sensitivity data, yielding purity and concentration information.

However, Raman observations of these products is particularly challenging at low concentrations (mg/ml), due to the weak scattering cross section of the target samples. Furthermore, many complex biological substances, e.g. antibody fragments, demonstrate very strong fluorescence responses which typically mask the Raman signature thereby hampering the application of Raman spectroscopy as an on-line PAT tool.

The number of approved monoclonal antibody-based biopharmaceutical products for a range of therapies continues to develop rapidly, including the recent development of Ronapreve

and Sotrovimab treatment for Covid-19. Despite these successes, antibody production is still burdened with challenges that impact both time and cost of development. Monoclonal antibodies and antibody fragments are expensive and any system that can provide data to improve their production is of interest. Antibody fragments (e.g., Fab, scFv, Dab, etc.) are an increasingly important class of protein-based biotherapeutics. Due to their structure and smaller size, antibody fragments possess advantageous properties (e.g., easier tissue penetration) that suit a range of diagnostic and therapeutic applications. They are, however, difficult to measure in low concentrations with the required high degree of specificity to improve their manufacture and increase yield. Thus, new or improved Process Analytical Technologies (PAT) are of significant interest.

Deep UV resonant Raman spectroscopy (UVRRS) has been explored by several authors as a potential approach to monitor the manufacture of biopharmaceutical products [1,2,3]. At < 250 nm operation, the target Raman and fluorescence response becomes spectrally separated, allowing samples to be analysed in detail. Further, as the laser wavelength reduces below 250 nm, it approaches the electronic transition of several organic molecules producing a resonant effect that can amplify the Raman signal by several orders of magnitude [4,5,6].

Current high-performance deep UV instruments use gas pumped lasers [4,5], which must be water cooled, and dry nitrogen purged, making them difficult to deploy in a manufacturing facility. An alternative approach is to use a CuNe laser as deployed on the Mars perseverance mission [7]. These lasers do not require cooling and are relatively compact. However, these lasers are pseudo pulsed with a net power of <<1 mW, which limits their application to strongly scattering or highly concentrated samples.

These instruments are typically coupled to a high-performance dispersive spectrometer and a cooled CCD. The resolution requirements to achieve good quality Raman spectra at laser wavelengths below 250 nm result in the spectrometer being sensitive to environmental conditions, thus often requiring regular realignment. This can result in the instrument requiring a larger physical footprint than when operating at longer wavelengths [1,2]. The spectrometer will typically use a 25 μm (or less) slit to ensure the spectra is well-resolved. To ensure the maximum light collection in this arrangement, the laser spot at the target needs to be kept below this slit width, resulting in the target sample being exposed to large power densities, which together with the high photon energy can lead to sample damage [8,9]. Further, the resolution requirements to achieve good quality Raman spectra at laser wavelengths below 250 nm result in the spectrometer being sensitive to environmental conditions, thus often requiring regular realignment.

These challenges have, to date, limited the adoption of deep UV Raman instruments to academic laboratories and very specific research applications such as Mars exploration missions. The ancillary requirements and high running costs have also severely limited the deployment of UVRRS systems as on-line PAT tools, where biologics manufacturing could be facilitated and enhanced.

To address these issues the ISI and TOPTICA have developed a new compact deep UV Raman instrument using a diode pumped laser and a spatial heterodyne spectrometer (SHS) [10] combined with an all-reflective Raman collection probe. The diode laser allows the instrument

to maintain a compact form, whilst yielding excellent stability and performance characteristics. The SHS allows for a large optical throughput resulting in a comparably large laser spot at the target thereby mitigating against power density-induced sample damage.

The instrument has been demonstrated to successfully capture the Raman spectra of a range of biochemical samples, including immunoglobulin (IgG) at varying concentrations, tryptophan, and a series of domain antibody (dAb) samples. The dAb samples were extracted at different stages of a pilot bioreactor manufacturing process and at varying dilutions. To the knowledge of the authors, this is the first time an observation of this type has been made.

2. Experimental / Instrument development

A CAD image of the instrument (with enclosure removed) is presented in Fig1.

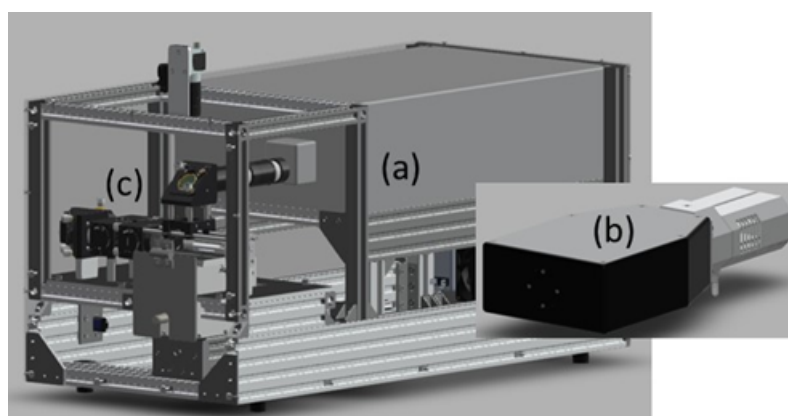


Fig 1. CAD image of full system: (a) TOPTICA laser head, (b) ISI HES spectrometer and (c) backscatter Raman collection probe

The system consists of (a) a diode laser manufactured by TOPTICA Photonics, (b) a spatial heterodyne spectrometer and (c) reflective Raman collection probe, both produced by IS-Instruments. The main instrument has a form factor of $75 \times 45 \times 35$ cm and interfaces to the spectrometer via fibre optic cable.

2.1 Laser

A new deep-UV laser system, operating at 228.5 nm was developed by TOPTICA Photonics (Fig 1a), which crucially required neither water cooling nor internal gas purging thereby substantially simplifying operation. This laser source was optimized for a compact footprint and is based on diode-pumped solid-state laser (DPSSL) technology. The DPSSL is used as a low-noise pump laser, providing an output power of around 200 mW at the fundamental wavelength of 457 nm. This is frequency-converted into the deep-UV using the process of second-harmonic generation (SHG). The necessary output power of > 10 mW in the UV is

achieved by combining the SHG process with an optical enhancement cavity, which allows for a conversion efficiency of more than 13 % and a maximum UV power of 20 mW.

Optical components used in the UV stage of the laser, especially the non-linear crystal, are prone to UV induced degradation, therefore the full UV compartment is hermetically sealed to ensure stable operation in target deployment environments. To further extend the lifetime, the UV compartment is equipped with an optics shifter, which can move the nonlinear crystal (without manual alignment) inside the cavity and provides multiple spots of operation on the crystal surface. With a measured spot lifetime of more than 1,000 hours, the UV laser meets industry requirements for lifetime of > 10,000 hours.

Additionally, an optical lens system for UV beam shaping is part of the sealed compartment. This system includes lenses to focus the UV beam into an optical slit, where walk-off induced features of the beam profile are blocked, resulting in an output beam quality of $M^2 < 1.3$. This beam profile ensures an optically clean and small focus at the target samples. Using two additional lenses, the output beam is slightly focussed, so that the focus position is 0.7 m from the laser aperture and the $1/e^2$ beam diameter is around 200 μm . With these beam parameters, no external lens is needed to measure samples with the Raman instrument.

2.2 Sample Interface

The Raman collection probe is an all-reflective device, where the laser is directed at the sample via a turning mirror which directs the light down at the sample as shown in Fig2.

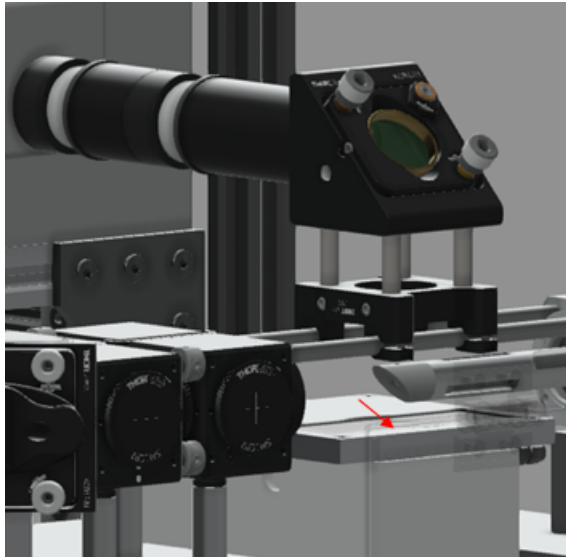


Fig 2. CAD image of the instrument – sample interface. Red arrow indicates sample position.

The position of the sample is indicated with a red arrow. The backscattered Raman light is collected via a 12.5 mm focal length f1:1 mirror. The light is then passed through a 229 nm long pass filter to suppress extraneous laser light before focussing into a 0.91 mm diameter collection fibre, via a 25 mm diameter, 50 mm focal length mirror. The light is then fibre coupled into the spectrometer where the spectral information is extracted. The SHS spectrometer design ensures no light is lost despite the large etendue requirements. [11]

A dynamic positioning stage on which the sample is sited is also shown in Fig2 (below sample stage). This facilitates a scanning routine throughout the duration of the Raman measurement ensuring the samples were not damaged by prolonged laser exposure, a function presented and discussed in detail in the Results and Discussion section.

2.3 Spectrometer

The spectrometer has a spatial heterodyne configuration as shown in Fig3.

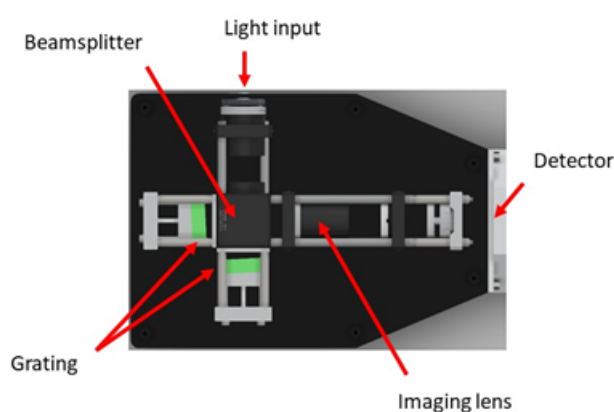


Fig 3. Spatial heterodyne spectrometer design as used by the UVRRS instrument

The design lends itself well to operation in the deep UV, where resolution, power density and stability requirements are very stringent.

This design was originally developed by Harlander et al (1992), to study diffuse stellar objects. Several teams have adapted the design for Raman observations at a range of excitation wavelengths [12,13,14]. The instrument is a class of static Fourier transform spectrometer and thus images an interferogram which must undergo a Fourier transform to extract the spectral information.

The design provides several advantages; it offers a significant etendue advantage over dispersive systems, this allows the spot at the target sample to be increased, reducing the power density, while losing no collected light. The interferometer configuration allows high resolution to be achieved with modest grating line densities with no requirement for increasing the instrument footprint. The design is inherently stable in wavelength space reducing any need for regular realignment of the instrument.

The spectrometer was fibre coupled to the Raman probe via a 0.91 mm diameter 0.22 NA optical fibre. The spectrometer requires no slit thereby eliminating this common source of optical loss. The instrument uses 400 lines/mm gratings, the fringe pattern is imaged via a triplet UV lens (to minimise aberrations) using a cooled Andor iDUS CCD camera.

Lamsal [15] demonstrated a UV SHS instrument using a split plate beam splitter to limit any distortion arising from plate flatness. However, this extends the distance between the gratings and other optical elements, which amplifies any movement in the grating plates due to environmental conditions. Therefore, a bespoke cubic beam splitter with a flatness of $\lambda/10$ at 228.5 nm was fabricated and incorporated into the instrument.

The spectrometer was calibrated using cyclohexane which exhibits a series of well-known discrete peaks from 801 cm^{-1} to 1444 cm^{-1} .

3. Results and Discussion

The spectrometer was calibrated using cyclohexane which exhibits a series of discrete peaks from 801 cm^{-1} to 1444 cm^{-1} as shown in Fig 4. Cyclohexane spectra were routinely acquired to confirm instrument stability was maintained.

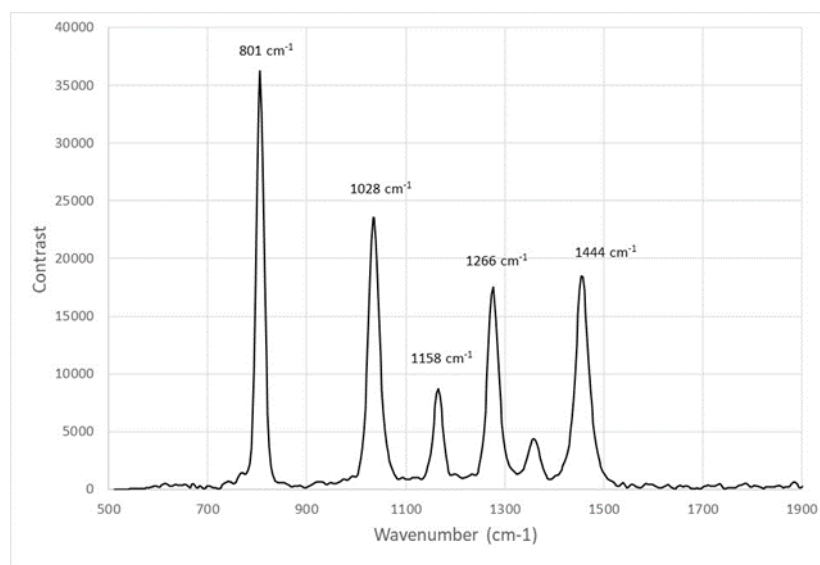


Fig 4. Raman spectrum of cyclohexane captured in 1s

3.1 IgG and Tryptophan

Whilst operating in the deep UV, target samples can experience very high radiant energies. This can result in degraded spectra being obtained as the target material is itself degraded and/or damaged. To assess this effect, IgG, which is known to be prone to UV degradation, was examined. This data was acquired using 30-second integration times where an average of 10 frames was used to produce the presented spectra.

IgG spectra were obtained in three different measurement conditions:

- Static; such that the same region of sample was continuously exposed to the laser
- Rotating; with the sample rotating, tracing an approx. 15mm circle over the sample surface
- Rotating and linearly translating as above with the addition of a 15mm 'to-and-fro' linear motion to ensure no region of the sample was exposed to extended laser light.

The resulting spectra are shown in Fig 5.

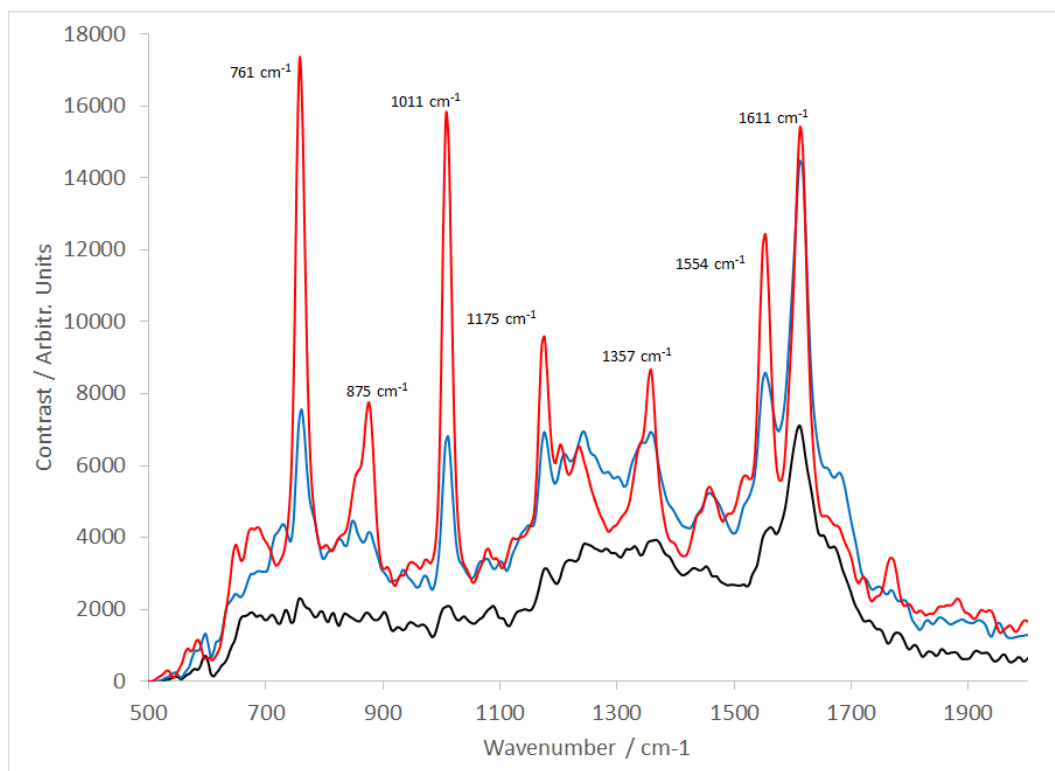


Fig 5. Raman spectra of IgG (30 second integration time, average of 10 frames). Solid black line: IgG is measured in static configuration; Blue line: IgG measured with sample rotating during the observation; Red line: IgG measured with a complex motion applied using a rotation and linear stage

In the static configuration, the spectra indicate a considerable amount of damage has occurred to the sample, with no clear peaks being present between 700 cm⁻¹ and 1500 cm⁻¹. Using a rotation stage improves the quality of the data obtained with peaks now becoming prominent in this region however they are 2-3 times weaker than the structure observed at 1605 cm⁻¹. The addition of the linear translation considerably enhances the spectral quality indicating no damage is observed within the timeframe of the measurement. This complex motion was adopted for all remaining samples presented. The spectra obtained under rotating-only circumstances replicates closely what is reported in the literature [16] indicating previous measurements may have been influenced by UV induced sample degradation.

Furthermore, a series of IgG dilutions in deionised water were produced. These ranged from 0.1 mg/ml to 2 mg/ml (11 samples in total). A subset of these is presented with Fig6.

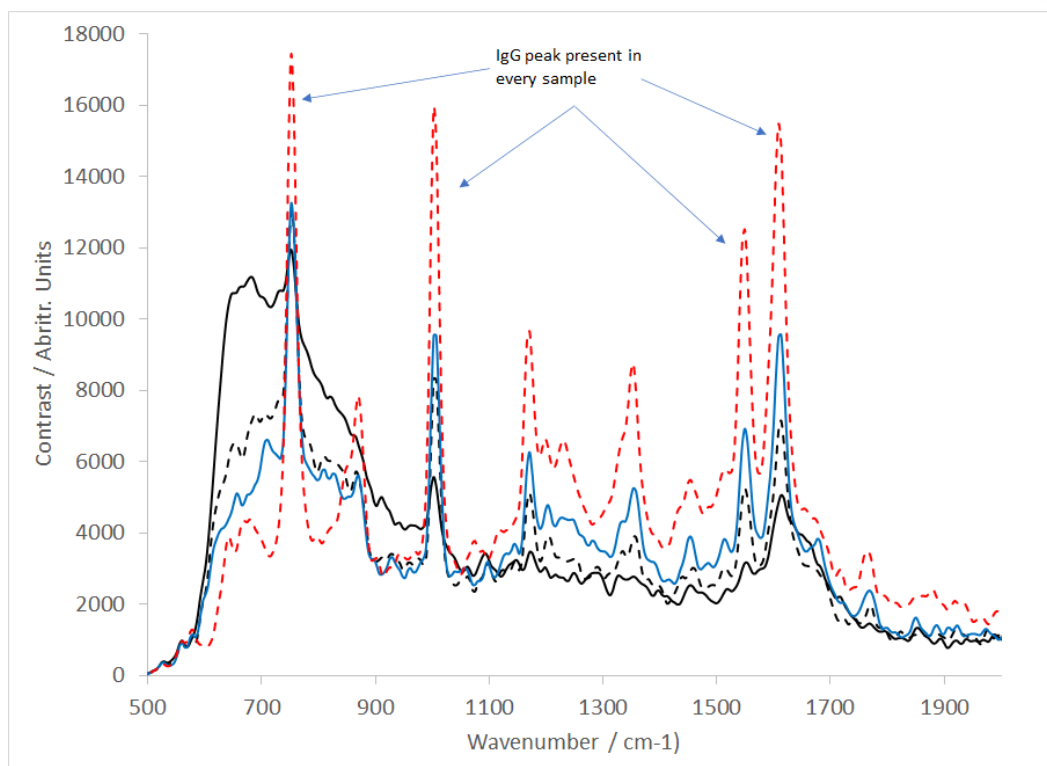


Fig 6. Raman spectra of IgG at a range of concentrations as labelled (all spectra presented are the averaged output of 10x 30 second frames); Solid black line = 0.1 mg/ml, dotted black line = 0.4 mg/ml, blue line = 0.8117 mg/ml, dotted red line = 2.0173 mg/ml

All spectra are the product of 10 averaged frames, each captured in a 30s integration time. The spectra illustrate that as the IgG concentration reduces towards 0.1 mg/ml the water spectrum becomes more prominent. Extrapolation indicates a detection limit of IgG in water of 0.08 mg/ml.

To determine the potential of the instrument for quantitative analysis, the spectra was further analysed using a Principal Component Regression model. This used a single 30s frame of each sample spectra, where the data was split into a training and a data set, using the K-folds cross validation technique [17]. A principal component analysis was then completed. The resultant output yielded the calculated IgG concentration values. This was plotted against the actual concentrations as shown in Fig 7.

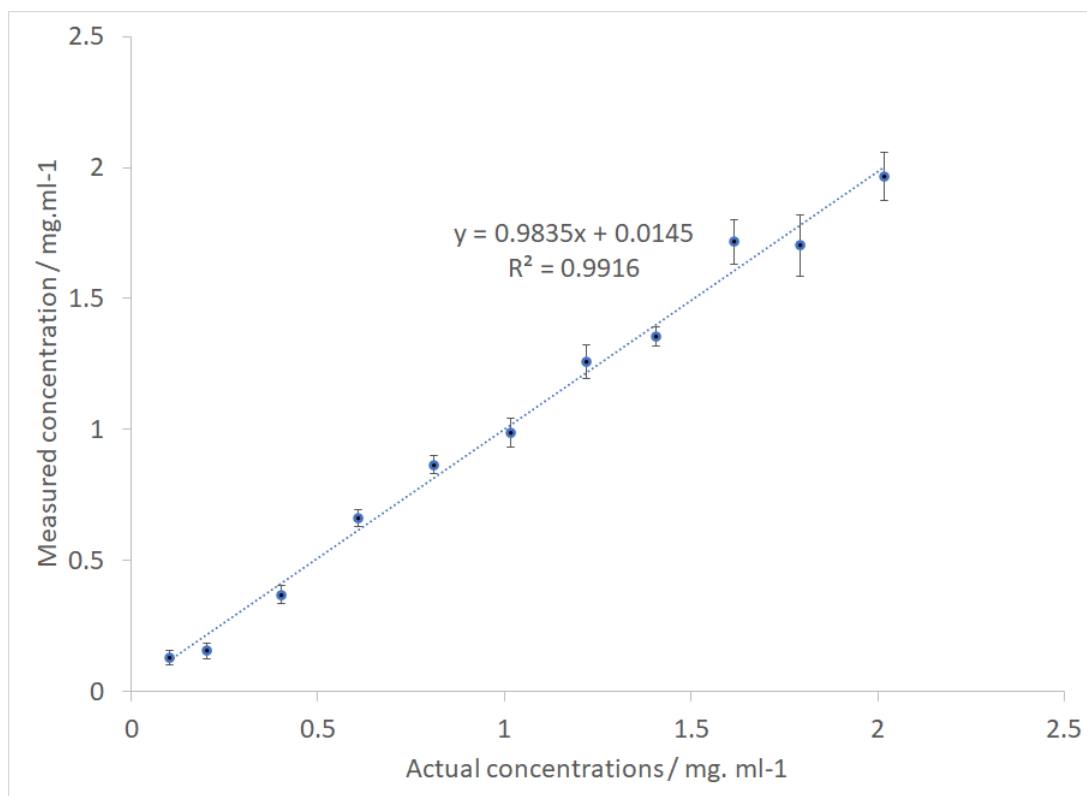


Fig 7. IgG PCR-calculated vs. actual sample concentration

The error bars are computed from the standard deviation of the individual frames with accuracy levels varying from 0.03 mg/ml for the low concentration sample to 0.1 mg/ml for the higher concentration samples. The data shows an excellent linear relationship with a regression coefficient of 0.99.

To further assess instrument utility, the common amino acid, tryptophan was examined. The Raman spectrum of this sample was acquired by averaging 10 frames, each captured in a 30 second integration time and is shown in Fig 8.

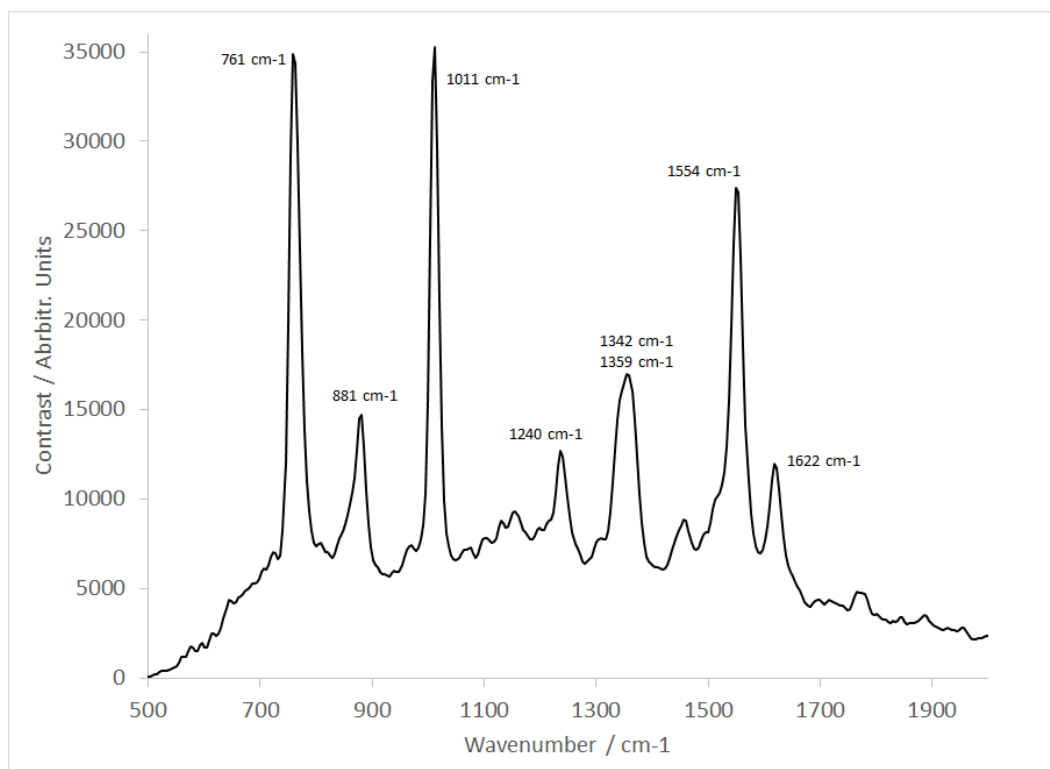


Fig 8. Raman spectrum of tryptophan

The sample concentration was 1.038 mg/ml and the sample was rotated and linearly translated to avoid sample degradation as detailed previously.

The interferogram produced by the spatial heterodyne spectrometer undergoes minimal processing prior to the FFT algorithm. This comprised of flat field correction to remove instrument aberrations, and a spline fit to remove the fibre intensity profile. No spectral smoothing has been applied.

Kumamoto et al. [8] has previously presented a well-resolved tryptophan Raman spectrum using a 2 cm⁻¹ resolution monochromator at 244 nm using a gas pumped laser. The spectrum in Fig7 compares well, with all peaks resolved, including the double peak at 1342 cm⁻¹ / 1359 cm⁻¹. However, in contrast, this spectrum was acquired in a fraction of the timeframe due to the advanced SHS technology replacing the scanning monochromator described in [8].

3.2 Domain antibody (dAb) Raman acquisition

A series of domain anti-bodies (dAb) supplied by Cytiva Life Sciences within the TESTA challenge programme [18] were also examined. The dAb pilot production facility at the TESTA centre, Uppsala is a technology demonstrator developed to support market innovation and promote Cytiva's products e.g., resins, filters, bioreactors etc. The process is intended to produce and purify a domain antibody fragment, i.e., the variable region of an antibody's kappa light chain. Antibody fragments used in diagnostic or therapeutic applications would be

produced in a similar fashion although with more rigorous routines (GLP or GMP standard) and have the end-product purified to an even higher degree.

Five samples obtained from different parts of the purification process were extracted and stored at -20°C for subsequent analysis with the deep UV Raman instrument. A list of the samples is shown in table 1.

Tab 1. List of dAb samples

	Sample	Description	Comment
1	End of Fermentation	Sample of Supernatant at harvest (heat treated to disrupt periplasm and release dAb)	Crude sample with a lot of contaminants (host cell proteins and DNA, culture media components etc.)
2	Protein L load	Sample taken after clarification step (TFF using Hollow fiber) before chromatography capture step (protein L resin)	Cell debris and large sized contaminants removed. Exchange of buffer.
3	Protein L pool	Sample from pooled fractions of protein L chromatography capture step	Protein L is the major purification step (affinity resin)
4	Capto MMC impres load	Should in principle be the same as protein L pool but might be in different buffer?	
5	Capto MMC impres pool	Sample after multimodal chromatography (polishing) step	Polishing step with further removal of endotoxins and host cell proteins (named ECP in diagram below)

Each of these samples was measured in the identical fashion to the IgG and tryptophan observations. The resulting spectra are displayed within Fig9.

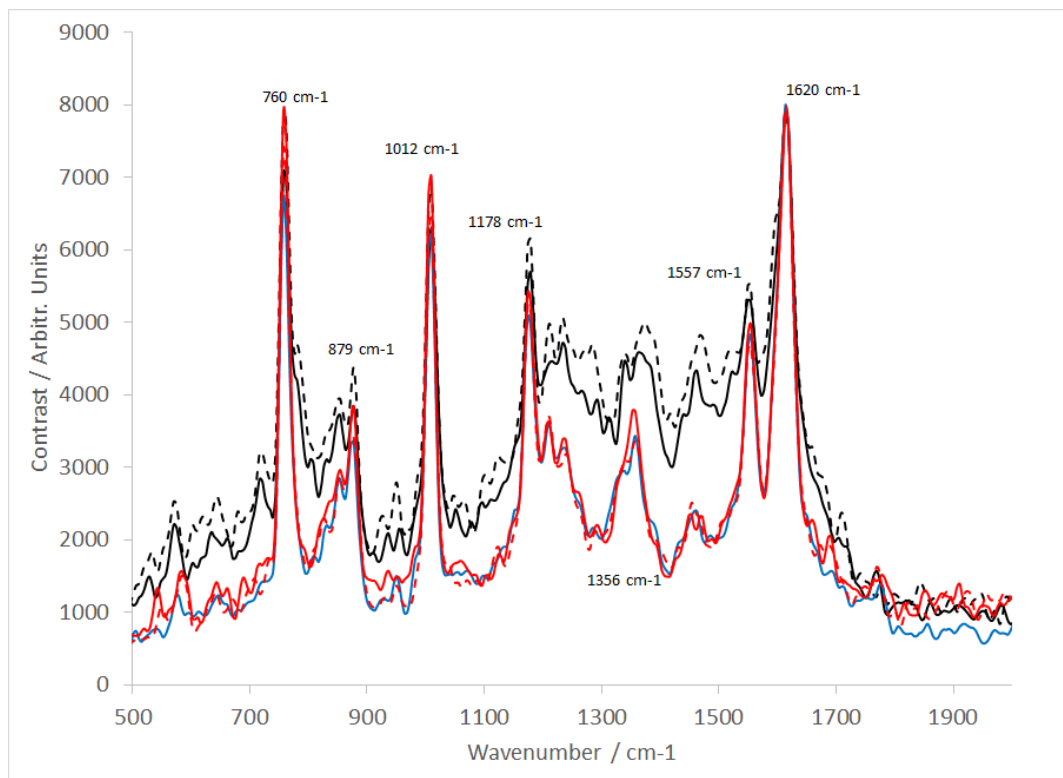


Fig 9. Raman spectra of dAb (sample provided by the TESTA Centre, Cytiva Life Sciences) taken from five different stages of the manufacturing process (Tab. 1): Dotted black line (sample position 1), solid black line (sample position 2), blue line (sample position 3), dotted red line (sample position 4), and solid red line (sample position 5)

Clear differences are observed between the early-stage process samples; samples labelled ‘end of fermentation’ and ‘Protein L load’ and the subsequent purification steps. Subtle differences are also visible between the remaining samples in terms of relative peak heights across the spectrum. This is likely due to the different dAb concentrations within each sample.

Furthermore, a sensitivity assessment was conducted. A series of capto L pool dAb samples were diluted into 5 different concentrations as detailed in Table 2.

Tab 2. dAb dilutions

<i>Dilution</i>	<i>dAb conc. (mg/mL)</i>	<i>Sample volume (μL)</i>	<i>Buffer volume (μL)</i>
100x	~0.1	20	1980
20x	~0.5	50	950
10x	~1	100	900
2x	~5	500	500
1x	~10	1000	0

The Raman spectra is presented in Fig10.

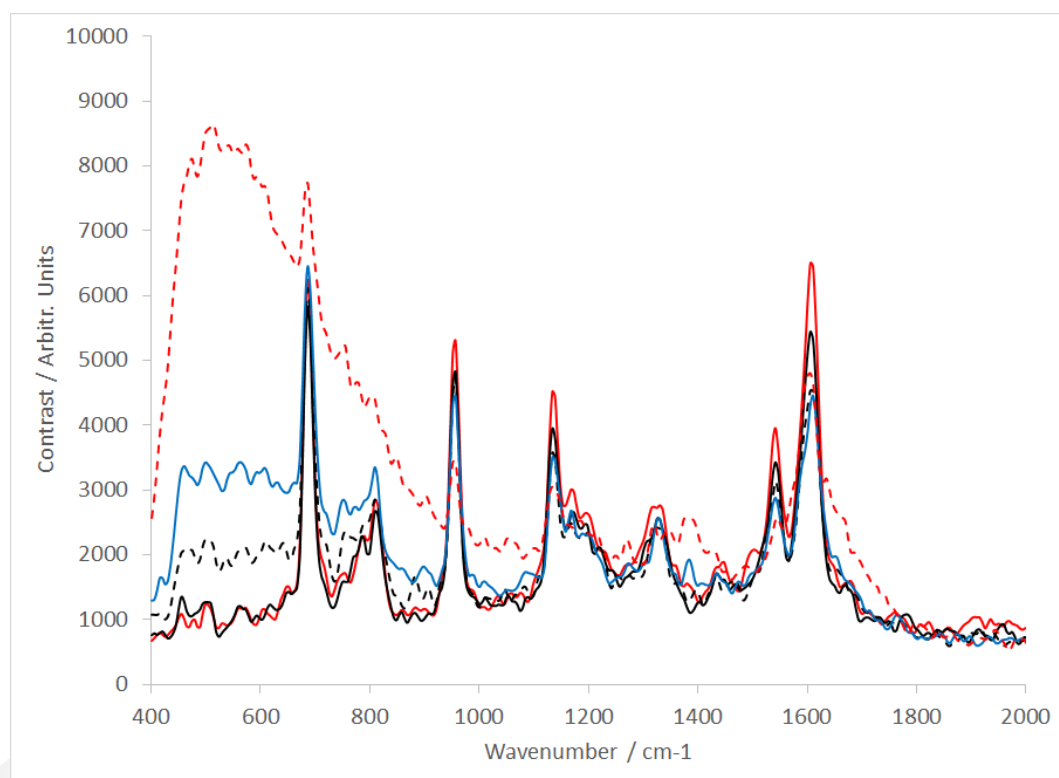


Fig 10. Raman spectra of dAb (sample provided by the TESTA centre, Cytiva Life Sciences) of different concentration levels: dotted red line = 0.1 mg/ml, solid blue line = 0.5 mg/ml, dotted black line = 1 mg/ml, solid black line = 5 mg/ml and solid red line = 10 mg/ml

Each spectra presented is the average of 10 frames, where each frame was captured in a 30 second integration time. In the low concentration samples, the solvent (PBS – predominantly water) can be observed, both at 1628cm^{-1} and below 1000cm^{-1} where the spectra rise steadily to the edge of the spectral range of the instrument. As the concentration increases, not only does the water feature become eliminated but the unique dAb peaks become more prominent.

The PCA analysis developed for the IgG data was repeated for the dAB data. A plot showing calculated vs. actual concentration is shown in Fig11.

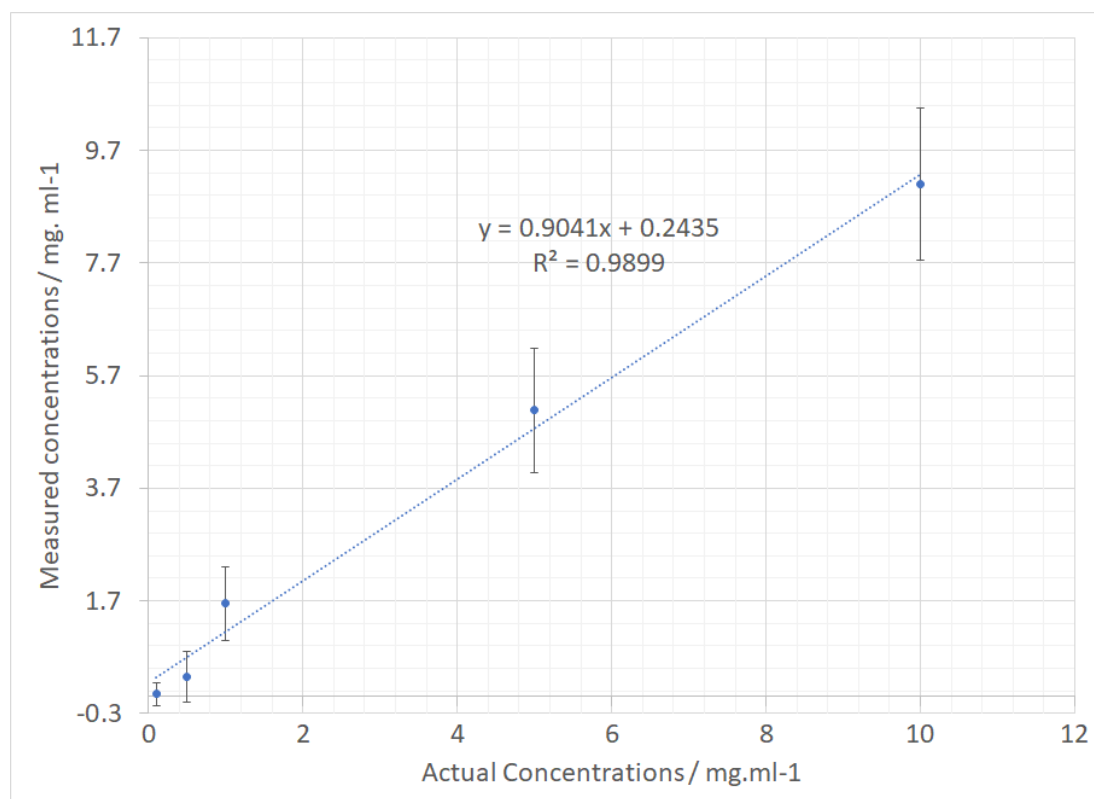


Fig 11. dAb PCR-calculated vs. actual sample concentration

Excellent linearity is again observed with a regression coefficient of 0.989. The error bars on the individual samples are larger due to the limited number of sample points across the concentration range. It is anticipated that in a manufacturing facility deployment scenario an increased number of samples could be used to construct a calibration model and thus improve individual measurement confidence. Furthermore, the analysis could be enhanced by using the full 300-second dataset rather than using a single 30second frame.

4 Conclusions

A new, compact, and reliable deep UV resonant Raman instrument has been presented. The system combines a newly developed solid state diode laser and a spatial heterodyne spectrometer integrated into a single instrument with a unique all-reflective backscatter

Raman collection probe. Sample damage caused by extended laser exposure has been mitigated via the introduction of a dynamic sample positioning stage.

Several biological materials have been studied using the UVRRS instrument: immunoglobulin, tryptophan, and domain antibodies. Each sample has yielded a unique and prominent Raman spectrum. Samples of varying concentration have also been examined, where excellent linearity characteristics demonstrated the utility of the instrument for quantitative analysis. A detection threshold <0.1mg/ml for IgG was determined.

A series of domain antibodies manufactured by the TESTA centre, a bioprocess pilot-scale technology showcase and innovation facility, run by Cytiva Life Sciences were successfully characterised. This exemplified the potential of the technology to monitor a biotechnology production process, while simultaneously determining sample concentration. This highlights the potential of the instrument to enhance production yield and reduce wastage.

6 References

- [1] L Ashton and R Goodarce (2011) European Pharmaceutical review Vol 16 Issue 3
- Wen, Z.-Q., Cao, X. and Vance, A. (2008). *J. Pharm. Sci* 97, 2229-2241
- [2] S, I. M., I, R., Rodrigues-Mendieta, Friel, C. T., Radford, S. E. and Smith, D. A. (2006). *Rev. Sci. Instrum* 77,055105
- [3] Smith, E. and Dent, G., (2005) *Modern Raman Spectroscopy - A Practical Approach*. John Wiley and Sons
- [4] S. Nocentini and L. Chinsky, *J. Raman Spectrosc.* 14(1), 9–10 (1983)
- [5] Y. Yazdi, N. Ramanujam, R. Lotan, M. F. Mitchell, W. Hittelman, and R. Richards-Kortum, *Appl. Spectrosc.* 53(1), 82–85 (1999)
- [6] Rohit Bhartia et al. (2021) *Space Science Rev* 217:58
- [7] Y. Kumamoto, A. Taguchi, N. Isaac Smith, and Satoshi Kawata (2011) *Biomedical Optics Express* Vol2 Issue 4
- [8] M. Harz, M. Krause, T. Bartels, K. Cramer, P. Rösch, and J. Popp, *Anal. Chem.* 80(4), 1080–1086 (2008)
- [9] J. Harlander, R. J Reynolds and F. L. Roesler., *Astro Phys Journal* 396 (1992)
- [10] M. Foster, M. Wharton, W. Brooks, M. Goundry, C. Warren and J. Storey (2020) *Journal of Raman spectroscopy* 51 2543-2551
- [11] J. E. Lawler, Z. E. Labby, J. M. Harlander, and F. L. Roesler, *Appl. Opt.* 47, 6371–6384 (2008)
- [12] O. R. Dawson and W. M. Harris, *Appl. Opt.* 48, 4227–4238 (2009)
- [13] M. J. Foster, J. Storey and M. A. Zentile *Optics Express* 2017; 25.
- [14] Lamsal, N., (2016) Univ. of S. Carolina, The Development of a high resolution deep-UV spatial heterodyne Raman spectrometer MSc Thesis
- [15] Plakhotnik, T., Reichardt, J., (2017) *Journal of Quantitative Spectroscopy and Radiative Transfer* 194, 58-64
- [16] Jolliffe, I. T. (1986). [Springer Series in Statistics] *Principal Component Analysis || Principal Components in Regression Analysis.* , 10.1007/978-1-4757-1904-8(Chapter 8), 129–155. doi:10.1007/978-1-4757-1904-8_8
- [17] <https://testa-challenge.confetti.events/>
- [18] J. Liu, M. Osadchy, L. Ashton, M. J. Foster, C. J. Solomon, S. Gibson, *Analyst* 2017, 142, 4067.

For more information visit

www.is-instruments.com

